Vol. 40, No. 1 (2018) 108-116, DOI: 10.24874/ti.2018.40.01.10

Tribology in Industry

www.tribology.rs

RESEARCH

Mathematical Modelling and Optimization of the Compressive Strength, Hardness and Density of a Periwinkle-Palm Kernel and Phenolic Resin Composite Brake Pad

B. Dan-asabe[a], A. Stephen[a]

[a]*Department of Mechanical Engineering, Ahmadu Bello University, Zaria, Nigeria.*

Keywords:

Periwinkle shell powder
Composite brake pad
Mathematical model
Quartic model
Palm kernel shell powder
Compressive strength
Mixture design

Corresponding author:

Bashar Dan-asabe
Ahmadu Bello University, Samaru, Zaria, Nigeria.
E-mail: b.danasabe@abu.edu.ng

A B S T R A C T

A composite of periwinkle shell powder, palm kernel shell powder, phenolic resin and other additives was developed in a form of a pad. Specimen composite samples were produced by compression at a temperature of 140 ˚C and mixture design using Design Expert software was used to analyse and optimise the samples. Mathematical models of the compressive stength, hardness and density were developed and statistically validated. Comparison of the models with experimental results showed that the compressive strength suited best with the cubic model, the hardness fitted with quadratic while the density agreed with all the models but suited best with cubic model. Optimized formulation with an objective of maximization compressive strength and hardness and minimization of the density was determined at 10.02, 10.78, 59.20 and 20 % of periwinkle shell powder (filler), palm kernel shell powder (filler), phenolic resin (matrix) and additives respectively.

1. INTRODUCTION

Development of composite brake pad that maximizes compressive strength and hardness and minimizes wear and density is essential in terms of cost savings using natural fibres of plant origin and other synthetic materials while improving the safety on our high ways. The importance of brake pad is to transform the kinetic energy of a vehicle to heat energy via friction and ejecting the heat to the surrounding environment [1]. Over 2,000 different materials and their variants have been used in commercial brake components [2]. The first brake pad material composed of cotton material impregnated with bitumen solution was invented by Herbert Frood [3] in 1879 which led to the establishment of the first brake pad company known as Ferodo Company. Composite brake pad constituents' materials are composed of varied composition of abrasives, binders, friction modifiers, fillers and reinforcements [4,5].

A composite material basically consists of matrix and reinforcement/filler. Combinations of different matrices and or different

reinforcements have been used to develop hybrid composites [6]. Some recent works on development and characterization of polymeric composites brake pad have been summarized thus. Olabisi et al. [7] developed a composite brake pad using pulverized cocoa beans shells as filler and epoxy as binder. Ademoh et al. [8] developed a composite brake pad using maize husks as filler and epoxy as binder. Thiyagarajan et al. [9] determined the influence of thermal conductivity and thermal stability of non-asbestos semi-metallic disc brake pad as a necessary requirement for friction materials.

Mixture experiments are a special case of response surface experiments where the response depends on the proportions of the various components and not on absolute amounts. An example is the strength of an alloy which depends on the various constituents' metals. Design variable constituents must be nonnegative and add up to one [10,11]. A general regression function of a 3rd degree polynomial that can be fitted to experimental data with q number of factors is given in the following [12,10]:

$$Y = \sum_{i=1}^{q} b_i x_i + \sum_{i\le j}^{q}\sum^{q} b_{ij} x_i\, x_j + \sum_{i\le j}^{q}\sum^{q} b_{ij*} x_i\, x_j(x_i - x_j) + \sum_{i\le j\le k}^{q}\sum^{q}\sum^{q} b_{ijk} x_i\, x_j x_k \quad (1)$$

The response for a three component mixture (x_1, x_2 and x_3) using Sheffe's canonical polynomials can be evaluated in terms of linear, quadratic, cubic, special cubic, quartic and special quartic prediction models respectively as given in the following [10,13]:

$$y(x_i) = b_1x_1 + b_2x_2 + b_3x_3 \quad (2)$$

$$y(x_i) = b_1x_1 + b_2x_2 + b_3x_3 + b_{12}x_1x_2 + b_{13}x_1x_3 + b_{23}x_2x_3 \quad (3)$$

$$y(x_i) = b_1x_1 + b_2x_2 + b_3x_3 + b_{12}x_1x_2 + b_{13}x_1x_3 + b_{23}x_2x_3 + b_{123}x_1x_2x_3 + b_{*12}x_1x_2(x_1-x_2) + b_{*13}x_1x_3(x_1-x_3) + b_{*23}x_2x_3(x_2-x_3) \quad (4)$$

$$y(x_i) = b_1x_1 + b_2x_2 + b_3x_3 + b_{12}x_1x_2 + b_{13}x_1x_3 + b_{23}x_2x_3 + b_{123}x_1x_2x_3 \quad (5)$$

$$y(x_i) = b_1x_1 + b_2x_2 + b_3x_3 + b_{12}x_1x_2 + b_{13}x_1x_3 + b_{23}x_2x_3 + b_{*12}x_1x_2(x_1-x_2) + b_{*13}x_1x_3(x_1-x_3) + b_{*23}x_2x_3(x_2-x_3) + b_{1*23}x_1^2x_2x_3 + b_{12*3}x_1x_2^2x_3 + b_{123*}x_1x_2x_3^2 + |b_{12*}x_1x_2(x_1-x_2)^2 + b_{13*}x_1x_3(x_1-x_3)^2 + b_{23*}x_2x_3(x_2-x_3)^2 \quad (6)$$

$$y(x_i) = b_1x_1 + b_2x_2 + b_3x_3 + b_{12}x_1x_2 + b_{13}x_1x_3 + b_{23}x_2x_3 + b_{1*23}x_1^2x_2x_3 + b_{12*3}x_1x_2^2x_3 + b_{123*}x_1x_2x_3^2 \quad (7)$$

where the coefficients $b_1, b_2, b_3, b_{12}, b_{13}, b_{23}, b_{123}, b_{*12}, b_{*13}, b_{*23}, b_{1*23}, b_{12*3}, b_{123*}, b_{12*}, b_{13*}$ and b_{23*} are constants determined simultaneously with the experimental variables and characterized results.

Mixture experiments are widely used today in formulation experiments, blending experiments and marketing choice experiments where the goal is to determine the most preferred attribute composition of a product at a given price [14]. Many researchers have used mixture design, response surface methodology (RSM) and other statistical methods to design and model their experimental data. Dan-asabe et al. [15] modelled and optimized the properties of a hybrid composite using mixture design. Agunsoye et al. [16] investigated the use of Delonix regia (Dr) seed particles as reinforcement for polymeric recycled low density polyethylene (RLDPE) composite produced using compression molding and predicted the tensile property of the RLDPE/Dr particle composites using mono-variate regression model. Javier [17] analyses the choice of slack-variable regression model amongst others mixture design experiments models such as Scheffé model and Kronecker model.

Elkamel et al. [18] developed vigorous statistical models for predicting the flexural properties and specific gravity of wheat straw polypropylene composite (WSPPC) using constrained mixture design [19]. Chaw and Yap [20] optimized process variables of epoxy/organo-montmorillonite nano composite on flexural properties by response surface methodology. Obam [21] used the BASIC programming language to evaluate the accuracy of Sheffe's second degree and third degree models in predicting desired strength of hardened concrete for any given mix proportions. Kpodo [22] investigated the use of multiple component constraint mixture design for studying the effect of ingredient variations on the chemical

composition and physico-chemical properties of soy, peanut and cow milk. Other researchers have used mixture design experiment and response models in optimization of juices and food ingredients [23,24].

The research work involved statistical mixture design, characterization, mathematical modelling, analysis and optimisation of a composite brake pad. The composite constituent consist of phenolic resin as matrix, periwinkle and palm kernel shell as fillers and other additives that include abrasives and friction modifiers. Natural fibres of plant origins have lower densities and provide good specific properties, better insulating advantage and low energy consumption during their growth or processing [25,26].

2. EXPERIMENT

2.1 Materials and Methods

Materials

Materials used are periwinkle shell powder, palm kernel shell powder, phenolic resin and additives comprising of friction modifier (saw dust and calcium oxide) and abrasive (iron filings and aluminum oxide).

Preparation

Appropriate amount of phenolic resin and polishing agent measured in weight percentage (Table 1) were thoroughly mixed in a container. Ground periwinkle shell powder, palm kernel shell powder, friction modifier and abrasives all measured in weight percentage (Table 1) were thoroughly mixed homogenously and then transferred to a rectangular steel open mold of dimensions 120×60×7 mm. A counter mold (lid) was placed unto the open mold to allow impregnation of the binder into the fillers and other additives (friction modifiers and abrasives). The mold setup was then placed in between the platens of a compressive press and compressed to a pressure of 100 MPa at a temperature of 140 °C for five minutes. The composite sample was thereafter removed and cured in an oven at a temperature of 120 °C for eight (8) hours. The process was carried out for various weights of the periwinkle, palm kernel, phenolic resin and constant additives as shown in Table 1.

Table 1. Composition of the composite brake pad for the various samples A to E.

	Material	A (%)	B (%)	C (%)	D (%)	E (%)
Fillers	Periwinkle shell powder	5	10	15	20	25
	Palm kernel shell powder	5	10	15	20	25
Binder	Phenolic resin	70	60	50	40	30
Friction modifier	Saw dust	6	6	6	6	6
	CaO	2	2	2	2	2
Abrasives	Iron filings	10	10	10	10	10
	Al_2O_3	2	2	2	2	2
		100	100	100	100	100

2.2 Experimental Design

The design was conducted using Design Expert version software [13]. The factors or design input variables are (in weight percentage): periwinkle, palm kernel, phenolic resin and additives in accordance with a similar mixture design as employed by Dan-asabe [6] and Elkamel et al. [18]. The objective or response variable of interest is the best sample composition that provides the maximum compressive strength and hardness with minimization of density. Ranges were used to set up a constrained design of a four component mixture design of a user defined and all-constituent-blends [27] as follows:

$$5\ \% \leq x_1 \leq 25\ \% \quad (8)$$

$$5\ \% \leq x_2 \leq 25\ \% \quad (9)$$

$$30\ \% \leq x_3 \leq 70\ \% \quad (10)$$

$$x_4 = 20\ \% \quad (11)$$

where x_1, x_2, x_3 and x_4 are weight percentages of periwinkle, palm kernel shell powder, phenolic resin and additives respectively. Five design points (experimental runs) were considered with all having quadruplet blends. The actual experiment was replicated thrice and averaged results for compressive strength hardness and density are tabulated in Table 2.

The actual design points (in %) are converted to lower pseudo coordinates (L-pseudo coding) points using Eq. 12 [15,19] as shown in Table 3.

$$z_1 = \frac{x_1 - 5}{40}\ ;\ z_2 = \frac{x_2 - 5}{40}\ ;\ z_3 = \frac{x_3 - 30}{40} \quad (12)$$

Table 2. Design points of the mixture design at 20 % additives ($x_4 = 20$).

Actual Composition (%)			Compressive strength (MPa) $y(x_i): R_1$	Hardness (HRF) $y(x_i): R_3$	Density (g/cm³) $y(x_i): R_2$
x_1	x_2	x_3			
5	5	70	3.154	72.1	0.980
10	10	60	10.808	82.4	1.000
15	15	50	8.192	99.7	1.015
20	20	40	4.346	112.7	1.034
25	25	30	1.769	131.3	1.071

Table 3. Design points in L-pseudo coding at 20 % additives ($z_4 = 0$).

L-pseudo coding			Compressive strength (MPa) $y(z_i): R_1$	Hardness (HRF) $y(z_i): R_3$	Density (g/cm³) $y(z_i): R_2$
z_1	z_2	z_3			
0	0	1	3.154	72.1	0.980
0.125	0.125	0.75	10.808	82.4	1.000
0.25	0.25	0.5	8.192	99.7	1.015
0.375	0.375	0.25	4.346	112.7	1.034
0.5	0.5	0	1.769	131.3	1.071

3. CHARACTERIZATION

3.1 Compressive strength

This was determined using a Universal Testing Machine (EnerPac P-391) in accordance with ASTM D71372 [28]. Sample specimen dimensions of 20×20×13 mm³ were produced for the test. Compressive load was applied axially onto the specimen till it ruptured. The compressive strength was then determined using Eq. 13.

$$\sigma = \frac{F}{A} \quad \text{(MPa)} \tag{13}$$

where F = force, and A = cross-sectional area.

3.2 Hardness

The hardness test was carried out using the INDENTEC Universal Hardness Testing Machine with a steel ball as the indentor. The sample was first machined to a size of 30×25×13 mm³ and then grinded [6]. The sample was then inserted beneath the indentor and the hardness value taken at three points on the surface of the sample. The average of the values was then recorded.

3.3 Density

The density of the composite was determined by measuring the volume and mass of the composite sample. The mass was measured with the aid of a digital weighing balance machine [29]. The volume was found using Archimedes' principle. The density was determined from Eq. 14 as follows:

$$\rho = \frac{m}{V} \quad \text{(g/cm}^3\text{)} \tag{14}$$

4. RESULTS AND DISCUSSION

4.1 Statistical analysis, validation and modelling of experimental results

The summary statistics of the models from Design Expert Package are shown in Tables 4, 5 and 6. For the compressive strength (Table 4), the linear, quadratic models are ruled (poor models) due to lower R-squared and adjusted R-squared with negative predicted R-squared [19,30]. The quartic model has R-squared value of 100 % implying accurate prediction of the experimental points but unsuitable for prediction of new points outside of experimental data (zero adjusted R-squared and predicted R-squared values). However, the cubic model gives good values of R-squared and adjusted R-squared suitable for prediction within experimental point [31,32] and not outside the limit of the experiment (poor predicted R-squared). The statistical significance of the cubic model is fairly good at 13.27 % (greater than the acceptable 5 %) principally as a result of the low predictability of -64 % predicted R-squared. Nevertheless, the cubic model is satisfactory with adequate precision value of 13, greater than the minimum bench mark of 4 [13,33]. Additionally, its value of the standard deviation is small compared to the linear and quadratic models.

For the hardness (Table 5), the cubic and quartic models are ruled out because of poor predicted R-squared values of 56.58 and 0 respectively. [32] However, the quadratic model has the highest prediction variability of 98.32 % and adequate precision 42.21 with p-value within acceptable error value of 0.3 %. Standard deviation is the lowest with a value of 1.82. For the density (Table 6), interestingly, the linear, quadratic and cubic models could be used

predicts the experimental points but with the cubic having the highest prediction variability of 96.88 %. The cubic model also has a p-value error significant value of 1.1 % and highest adequate precision value of 170.245. Standard deviation of the cubic model is thus the lowest. Moreover, validation of the compressive strength (cubic), hardness (quadratic) and density (cubic) models could also be observed from Figs. 1, 2 and 3 where the slope of the model (predicted response) against experimental points passing through (or closely) all the points and approximating to unity.

The cubic model of compressive strength, quadratic model of the hardness and cubic model of the density are given respectively in L-pseudo coding in Eqs. 15, 16, and 17. The actual formulations (in %) can be converted to the L-pseudo coding using Eq. 12 and respective properties can be predicted using these equations:

$$R_1 = 114.85z_1 + 3.25z_3 - 222.25z_1z_2 - 246.17z_1z_2z_3 \quad \text{(cubic)} \quad (15)$$

$$R_2 = 226.41z_1 + 71.8z_3 + 71.16z_1z_2 + 29.87z_1z_2z_3 \quad \text{(quadratic)} \quad (16)$$

$$R_3 = 2.18z_1 + 0.98z_3 - 0.072z_1z_2 - 0.49z_1z_2z_3 \quad \text{(cubic)} \quad (17)$$

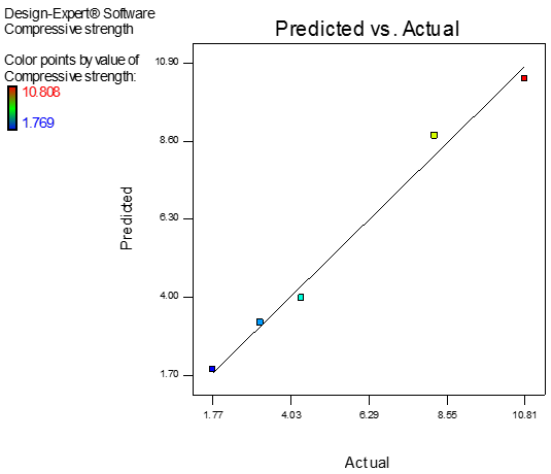

Fig. 1. Experimental vs. predicted results of the compressive strength (cubic model).

Table 4. Model summary statistics for compressive strength.

Source	Standard deviation	p-value	Adequate precision	R-Squared	Adjusted R-Squared	Predicted R-Squared
Linear	3.98	0.5164	1.467	0.1520	-0.1307	-2.4060
Quadratic	2.64	0.2480	3.936	0.7516	0.5032	-3.1753
Cubic	0.78	0.1327	12.258	0.9891	0.9564	-0.6418
Quartic	-	-	-	1	-	-

Table 5. Model summary statistics for hardness.

Source	Standard deviation	p-value	Adequate precision	R-Squared	Adjusted R-Squared	Predicted R-Squared
Linear	2.41	0.0003	39.025	0.9922	0.9896	0.9679
Quadratic	1.82	0.003	42.210	0.9941	0.9779	0.9832
Cubic	2.53	0.0683	26.121	0.9971	0.9885	0.5658
Quartic	-	-	-	1	-	-

Table 6. Model summary statistics for density.

Source	Standard deviation	p-value	Adequate precision	R-Squared	Adjusted R-Squared	Predicted R-Squared
Linear	0.00072	0.025	18.920	0.9597	0.9568	0.8742
Quadratic	0.00052	0.011	21.615	0.9890	0.9779	0.8094
Cubic	0.00006	0.011	170.245	0.9999	0.9997	0.9688
Quartic	-	-	-	1	-	-

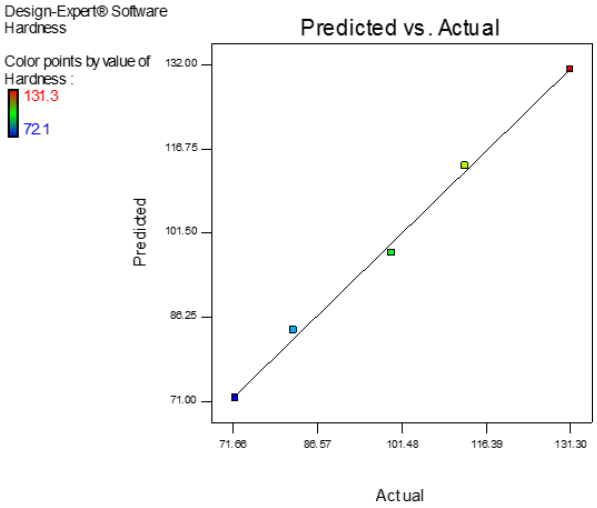

Fig. 2. Experimental vs. predicted results of the hardness (quadratic model).

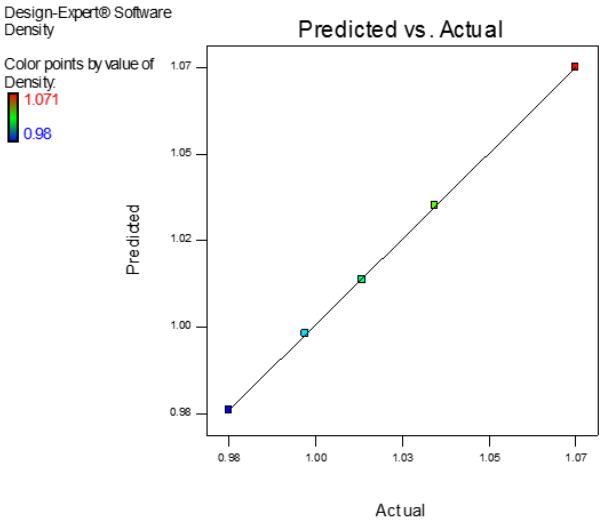

Fig. 3. Experimental vs. predicted results of the density (cubic model).

4.2 Response Optimization

The objective of a brake pad material is to maximize the compressive strength and hardness value and minimize the density [33]. The criteria for optimization are given in Table 7. The optimized model compositions plots of the compressive strength, hardness and density are respectively shown in Figs. 4, 5 and 6. The result of Figure 4 showed that the compressive strength was maximized (red graduated colour) at the percentage range for the respective periwinkle and palm kernel fillers of 8 – 30 % and at higher percentage of phenolic resin (40 – 68 %). Figure 5 showed that the hardness value increases as the percentage of the periwinkle and palm kernel increases and at lower percentage of the phenolic resin. Figure 6 showed that the density increases as the percentage of the periwinkle and palm kernel increases and at lower percentage of the phenolic resin. Conversely, the density was minimized at lower percentages of the periwinkle and palm kernel shell powders and at higher percentage of the phenolic resin.

Table 7. Optimisation criteria.

Material property	Objective criteria
Periwinkle (%)	Within range 5 to 25
Palm kernel (%)	Within range 5 to 25
Phenolic resin (%)	Within range 30 to 70
Additive (%)	Constant at 20
Compressive strength (MPa)	Maximise within range 4.65 to 10
Hardness (HRF)	Maximise within range 72.1 to 131.3
Density (g/cm^3)	Minimise within range 0.98 to 1

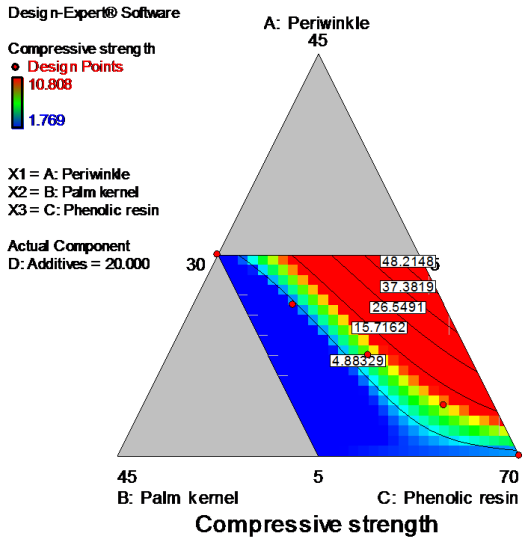

Fig. 4. Composition plot of the compressive strength.

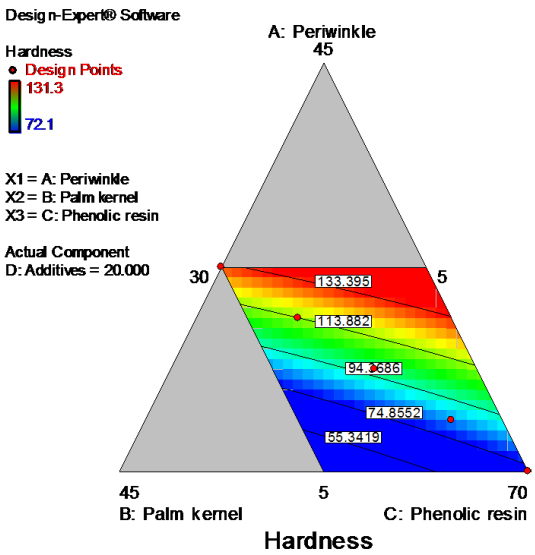

Fig. 5. Composition plot of the hardness.

Table 8. Optimization result.

Periwinkle (%)	Palm kernel (%)	Phenolic resin (%)	Compressive strength (MPa)	Hardnes (HRF)	Density (g/cm³)
10.02	10.777	59.202	10.443	83.265	0.98
10.445	11.277	58.278	10.411	83.485	0.98
10.743	11.629	57.628	10.353	83.758	0.98

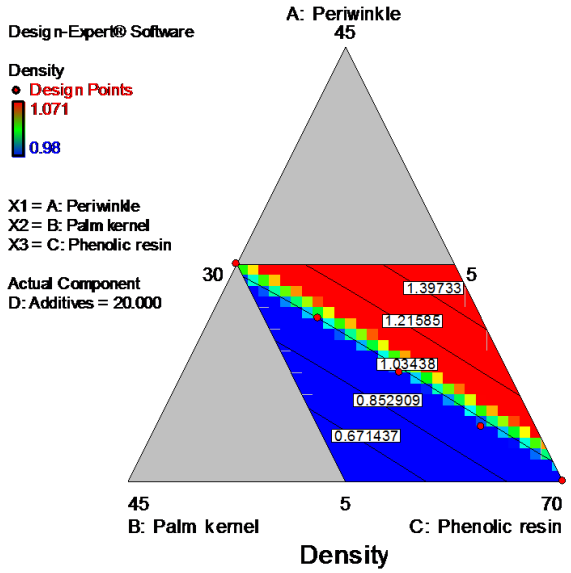

Fig. 6. Composition plot of the density.

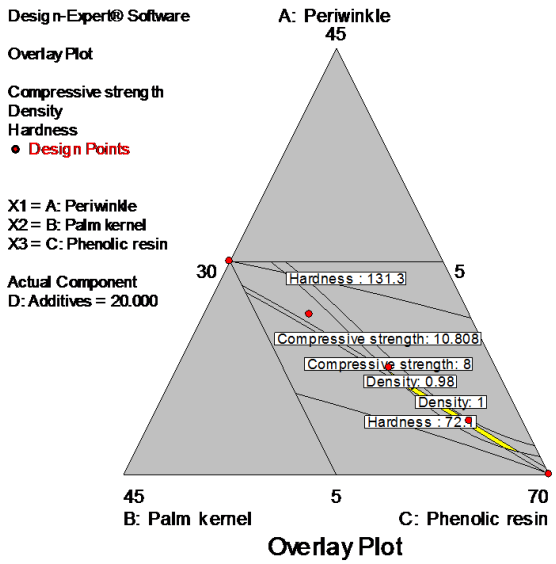

Fog. 7. Optimised overlay of formulations.

The result of the optimization was shown in Table 8 depicting three optimized formulation for the respective compressive strength, hardness and density. Either of the optimized formulations provides an optimum formulations since the response maximization of strength and minimization of density are approximately the same. The criteria of Table 7 was used to provide the overlay plot of Fig. 7 of the optimized region (shaded) of the compressive strength, hardness and density superimposed on one another. Any point within the shaded region is a desirable likelihood of the optimum formulation [33]. However, formulation with 10.02, 10.78, 59.20 and 20 % additives was selected the optimum best due to its higher desirability value of 0.894 as compared with 0.889 and 0.879 for the other formulation. This formulation corresponds to 10.44 MPa, 83.265HRF and 0.98 g/cm³ of the compressive strength, hardness and density respectively.

Additionally, the percentage water absorption after 3 number of days was determined as 0.49, 1.24, 1.14, 1.11 and 0.59 % for samples A, B, C, D and E respectively. The optimized sample is close to sample B (of 1.24 % water absorption). This can be used to infer a very low (negligible) porosity of the composites [34-36].

5. CONCLUSION

Results of the statistical modeling showed that cubic model suited well with the experimental result of the compressive strength and density while the hardness fitted well with the quadratic model. The compressive strength is useful in predicting experimental response and less meaningful in predicting new response giving significance error of 13.37 % (p-value). However, the hardness and density models are useful in predicting new formulations with prediction accuracy of 98.32 and 96.88 %. Validity of the models were confirmed using p-value, adequate precision and graphical plots of experimental and model values with slope approximating to unity. The optimization of the formulations was determined within the region of sample B.

RECOMENDATION

It is recommended that more number of design points should be used for the factors for increased precision of model prediction.

REFERENCES

[1] B. Dan-asabe, P.B. Madakson, J. Manji, *Material Selection and Production of a Cold-Worked Composite Brake Pad*, World Journal of Engineering and Pure and Applied Sci., vol. 2, no. 3, pp. 92-97, 2012.

[2] P.J. Blau, *Compositions, Functions, and Testing of Friction Brake Materials and Their Additives,* Oak Ridge National Laboratory, 2001.

[3] G. Nicholson, *Facts About Friction*, Gedoran, Winchester: P&W Price Enterprises, 1995.

[4] R.T. Spurr, *Fillers in Friction Materials*, Wear, vol. 22, iss. 3, pp. 367-409, 1972, doi: 10.1016/0043-1648(72)90395-X

[5] L. Gudmand-Hoyer, T.G. Bach, M. Per, *Tribological properties of automotive disc brakes with solid*, Wear, vol. 232, iss. 2, pp. 168-175, 1999, doi: 10.1016/S0043-1648(99)00142-8

[6] B. Dan-asabe, *Development of a Doum Palm Leaves/Banana Stem-Kankara Clay Hybrid Particulate Reinforced PVC Composite for Piping Applications*, PhD thesis, Department of Mechanical Engineering, Ahmadu Bello University, Zaria, 2017.

[7] A.I. Olabisi, A.N. Adam, O.M. Okechukwu, *Development and Assessment of Composite Brake Pad Using Pulverized Cocoa Beans Shells Filler*, International Journal of Materials Science and Applications, vol. 5, iss. 2, pp. 66-78, 2016.

[8] N.A. Ademoh, *Development and Evaluation of Maize Husks (Asbestos-Free) Based Brake Pad,* Industrial Engineering Letters, vol. 5, no. 2, pp. 67-80, 2015.

[9] V. Thiyagarajan, K. Kalaichelvan, R. Vijay, D.L., Singaravelu, *Influence of thermal conductivity and thermal stability on the fade and recovery characteristics of non‐asbestos semi‐metallic disc brake pad*, Journal of Brazillian Society Mechanical Science Engineering, vol. 38, iss. 4, pp. 1207-1219, 2016, doi: 10.1007/s40430-015-0448-8

[10] W.G. Oehlert, *A First Course in Design and Analysis of Experiments*, Library of Congress Cataloging-in-Publication Data, 2010.

[11] A.W. Shewhart, S.S. Wilks, *Experiments with Mixtures -Designs, Models, and the Analysis of Mixture Data*, New York: John Wiley & Sons, Inc., 2002.

[12] R.U. Owolabi, M.A. Usman, A.J. Kehinde, *Modelling and optimization of process variables for the solution polymerization of styrene using response surface methodology*, Journal of King Saud University - Engineering Sciences, vol. 30, iss. 1, 2018, doi: 10.1016/j.jksues.2015.12.005

[13] Stat-Ease, *Design-Expert® Software Version 10 Free Trial*, available at https://www.statease.com/software/dx10-trial.html, accessed: 20.06.2017

[14] J.B. Wiley, D. Ragavarao, P. Chitturi, *Choice-Based Conjoint Analysis Models and Designs*, New York: CRC Taylor & Francis Group, 2010, doi: 10.1201/9781420099973

[15] B. Dan-asabe, S.A. Yaro, D.S. Yawas, S.Y. Aku, *Statistical Modeling and Optimization of the Flexural Strength, Water Absorption and Density of a Doum Palm-Kankara Clay Filler Hybrid Composite*, Journal of King Saud University - Engineering Sciences, In Press, 2017, doi: 10.1016/j.jksues.2017.11.003

[16] J.O. Agunsoye, S. A. Bello, L.O. Kolawole, *Experimental Investigation and Theoretical Prediction of Tensile Properties of Delonix regia Seed Particle Reinforced Polymeric Composites*, Journal of King Saud University - Engineering Sciences, In Press, 2017, doi: 10.1016/j.jksues.2017.01.005

[17] C.S. Javier, *Selecting the Slack Variable in Mixture Experiment*, Selección de la variable de holgura en experimentos para mezclas, vol. 16, iss. 4, pp. 613-623, 2015, doi: 10.1016/j.riit.2015.09.013

[18] A. Elkamel, R. Fatoni, L. Simon, *Optimal Product Design of Wheat Straw Polypropylene Composites*, in 3rd International Conference on Industrial Engineering and Operations Management, 3-6, July, 2012, IEOM 2012, Istanbul, Turkey, pp. 2116-2126.

[19] R. Fatoni, *Product Design of Wheat Straw Polypropylene Composite,* PhD thesis, University of Waterloo, Ontario, 2012.

[20] W.S. Chow, Y.P. Yap, *Optimization of process variables on flexural properties of epoxy/organo-montmorillonite nanocomposite by response surface methodology*, eXPRESS Polymer Letters, vol. 2, no. 1, pp. 2–11, 2008, doi: 10.3144/expresspolymlett.2008.2

[21] S.O. Obam, *The accuracy of Scheffe's third degree over second-degree, optimization regression polynomials*, Nigerian Journal of Technology, vol. 25, no. 2, pp. 1-10, 2006.

[22] F.M. Kpodo, E.O. Afoakwa, B.B. Amoa, F.K.S. Saalia, A.S. Budu, *Application of multiple component constraint mixture design for studying the effect of ingredient variations on the chemical composition and physico-chemical properties of soy-peanut-cow milk*, International Food Research Journal, vol. 20, iss. 2, pp. 811-818, 2013.

[23] H.N. Sin, S. Yusuf, N.S.A. Hamid, R.A. Rahman, *Optimization of hot water extraction for*

sapodilla juice using response surface methodology, Journal of Food Engineering, vol. 74, iss. 3, pp. 352-358, 2006, doi: 10.1016/j.jfoodeng.2005.03.005

[24] A.J. Trevisan, J.A. Areas, *Development of corn and flaxseed snacks with high-fibre content using response surface methodology (RSM)*, *International Journal of Food Sciences and* Nutrition, vol. 63, iss. 3, pp. 362-367, 2012, doi: 10.3109/09637486.2011.629179

[25] F.Z. Arrakhiz, M.E. Achaby, C.A. Kakou, S. Vaudreuil, K. Benmoussa, R. Bouhfid, *Mechanical properties of high density polyethylene reinforced with chemically modified Coir fibers: impact of chemical treatments*, Material Design, vol. 37, pp. 379-383, 2012, doi: 10.1016/j.matdes.2012.01.020

[26] H. Essabir, E. Hilali, A. Elgharad, H.E. Minor, A. Imad, A. Elamraoui, *Mechanical and thermal properties of bio-composites based on polypropylene reinforced with Nut–shells of Argan particles*, Mater Des., vol. 49, pp. 442-448, 2013, doi: 10.1016/j.matdes.2013.01.025

[27] J. Cornell, *Experiments with Mixtures; Designs, Models, and the Analysis of Mixture Data*, New York: Wiley Inter-science, 2002.

[28] ASTM D7137, *Standard Test Method for Compressive Residual Strength Properties of Damaged Polymer Matrix Composite Plates*, 2012.

[29] ASTM D792, *Standard Test Methods for Density and Specific Gravity (Relative Density) of Plastics by Displacement*, 2013.

[30] H. Le Man, S.K. Behera, H.S. Park, *Optimization of operational parameters for ethanol production from Korean food waste leachate*, Int. J. Environ. Sci. Technol., vol. 7, iss. 1, pp. 157-164, 2010.

[31] A. Koocheki, A.R. Taherian, S. Razavi, A. Bostan. *Response surface methodology for optimization of extraction yield, viscosity, hue and emulsion stability of mucilage extracted from Lepidium perfoliatum seeds*, Food Hydrocolloids, vol. 23, iss. 8, pp. 2369-2379, 2009, doi: 10.1016/j.foodhyd.2009.06.014

[32] A. Rai, B. Mohanty, R. Bhargava, *Supercritical extraction of sunflower oil: a central composite design for extraction variables*, Food Chemestry, vol. 192, pp. 647-659, 2016, doi: 10.1016/j.foodchem.2015.07.070

[33] B. Dan-asabe, A.A. Galadi, *Mathematical Modeling of the Flexural Strength, Impact Energy and Water Absorption of a Pineapple Fibre-HDPE Composite using RSM Technique*, Journal of Polymer & Composites, vol. 5, no. 2, pp. 42-49, 2017.

[34] F.R. Gibson, *Principle of composite material mechanic,* Florida: US, CRC Press, 3rd edition, 2011.

[35] A.F. Angelin, R.C.C. Lintz, L.A. Gachet-Barbosa, W.R. Osório, *The effects of porosity on mechanical behavior and water absorption of an environmentally friendly cement mortar with recycled rubber*, Construction and Building Materials, vol. 151, pp. 534-545, 2017, doi: 10.1016/j.conbuildmat.2017.06.061

[36] Z.F. Farhana, H. Kamarudin, A. Rahmat, A.M. Mustafa Al Bakri, *The Relationship between Water Absorption and Porosity for Geopolymer Paste*, Materials Science Forum, vol. 803, pp. 166-172, 2015, doi: 10.4028/www.scientific.net/MSF.803.166